

See discussions, stats, and author profiles for this publication at: <https://www.researchgate.net/publication/259112362>

# Anisotropic Colloidal Micro-Muscles from Liquid Crystal Elastomers.

ARTICLE *in* JOURNAL OF THE AMERICAN CHEMICAL SOCIETY · JANUARY 2014

Impact Factor: 12.11 · DOI: 10.1021/ja410930g · Source: PubMed

---

CITATIONS

13

---

READS

122

4 AUTHORS, INCLUDING:



[Jean Elizabeth Marshall](#)

University of Cambridge

23 PUBLICATIONS 288 CITATIONS

SEE PROFILE



[Eugene M Terentjev](#)

University of Cambridge

304 PUBLICATIONS 7,485 CITATIONS

SEE PROFILE



[Stoyan K. Smoukov](#)

University of Cambridge

64 PUBLICATIONS 1,575 CITATIONS

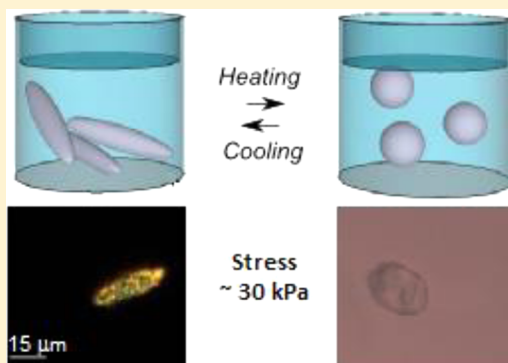
SEE PROFILE

## Anisotropic Colloidal Micromuscles from Liquid Crystal Elastomers

Jean E. Marshall,<sup>†</sup> Sarah Gallagher,<sup>‡</sup> Eugene M. Terentjev,<sup>‡</sup> and Stoyan K. Smoukov<sup>\*,†</sup><sup>†</sup>Department of Materials Science and Metallurgy, University of Cambridge, 27 Charles Babbage Road, Cambridge, CB3 0FS, United Kingdom<sup>‡</sup>Cavendish Laboratory, University of Cambridge, JJ Thomson Avenue, Cambridge, CB3 0HE, United Kingdom

## S Supporting Information

**ABSTRACT:** Monodomain liquid crystal elastomers (LCEs) are new materials uniquely suitable for artificial muscles, as they undergo large reversible uniaxial shape changes, with strains of 20–500% and stresses of 10–100 kPa, falling exactly into the dynamic range of a muscle. LCEs exhibit little to no fatigue over thousands of actuation cycles. Their practical use has been limited, however, owing to the difficulty of synthesizing components, achieving consistent alignment during cross-linking across the whole material and often a high nematic-isotropic phase transition temperature. The most widely studied method for LC alignment involves mechanical stretching of the material during one of two cross-linking steps, which makes fabrication difficult to control and lends itself mainly to samples that can be easily grasped (with sizes of the order of mm). In this article, we describe a method of adapting the LCE synthesis to microscale objects, achieving monodomain alignment with a single cross-linking step, and lowering the cycling temperature. LCE precursor droplets are embedded in and then stretched in a polymer matrix at high temperature. Confinement of the uniaxially stretched droplets maintains the alignment achieved during stretching and allows us to eliminate one of the cross-linking steps and the variability associated with it. Adding a comonomer during the polymerization leads to lowering of the nematic-to-isotropic transition temperature (58 °C), significantly expanding the range of potential applications for these micromuscles. We demonstrate reversible thermal switching of the micromuscles in line with the largest strain changes observed for side-chain LCEs and a differential scanning calorimetry characterization of the material phase transitions. The method demonstrates the parallel fabrication of many microscale actuators and is amenable to further scale-up and manufacturing.



## ■ INTRODUCTION

Liquid crystalline elastomers (LCEs) are unusual materials, capable of undergoing significant shape change (with uniaxial strain changes of up to 400–500%)<sup>1–3</sup> in response changes in their environment (temperature, radiation intensity). LCEs have the potential to be used as both sensors and actuators<sup>2,4–7</sup> and can generate stresses (~30 kPa)<sup>4</sup> that are useful for artificial muscles. LCEs are relatively soft and able to bend and conform to surfaces (Young's modulus of the order of 0.1 MPa).<sup>8</sup> They do not require an aqueous environment in which to expand/contract, unlike hydrogel actuators which require interaction of water with their molecular chains for operation. This makes LCE actuators attractive for operation in vacuum or anhydrous environments.

Thus far, the most reliable synthesis of LCEs has been achieved using the two-step method pioneered by Finkelmann and co-workers, which involves partial cross-linking of the material and mechanical stretching to induce alignment of the LC mesogens (rigid, anisotropic moieties capable of forming ordered LC phases) before a second cross-linking step.<sup>9</sup> Since this process requires the material to be mechanically grasped and stretched without breakage, significant limitations are imposed on the size/shape of components that can be made.

These are typically ribbon-shaped materials with length and width of the order of centimeters and thickness of the order of hundreds of micrometers.

For micromechanical systems, it would be advantageous if the process could be adapted so that LCE actuators can efficiently be made on a smaller scale. If no attempt is made to influence the LC ordering, then the result tends to contain several LC domains, whose diameter is of the order of micrometers. Since the average mesogen orientation varies between one domain and the next, the contraction of multiple domains is not coordinated in the same direction, and overall shape change in response to LC phase transitions is not remarkable in such a material. It is difficult to apply a controlled mechanical force to microscale objects; alternative approaches toward uniaxial LC alignment (without mechanical stretching) include electromagnetic fields and surface alignment/photopatterning. Keller and co-workers used a magnetic field to align the LC mesogens across a patterned sample, while exposing the material to UV in order to achieve polymerization and cross-linking.<sup>10</sup> Although it may be difficult to up-scale such a

Received: November 5, 2013

Published: December 2, 2013



technique, which is fundamentally limited to a surface, this method gives good LC alignment with a relatively low magnetic field; in contrast to other studies in which inconveniently high fields were required for LC alignment. In several of these cases, the fields required were either magnetic fields that are difficult to achieve with permanent magnets or electrical fields that are close to those capable of distorting or breaking down polymeric materials.<sup>11–13</sup> Surface alignment/photopatterning techniques can also create ordered LC materials;<sup>14–17</sup> however, questions remain as to their scalability, and patterning of the material tends to be carried out in two dimensions only (parallel to the surface). An interesting line of research, recently pursued by Zentel and co-workers,<sup>18</sup> relies on a microfluidic device to create droplets of LCE material, with shear flow during preparation being assumed to create the required LC alignment. The microfluidic technique allows the production of microscale LCE components to be scaled up significantly, but control over the LC alignment is limited since the fluid dynamics of a polymerizing droplet in a microchannel is quite complicated. In order for this field to progress, convenient methods must be found to scale up the production of free-standing LCE components, with good LC alignment across each component in order for the structures to show significant actuating strain during a phase transition.

Anisotropic microparticles are of considerable research interest on their own because they can potentially interact with the biological environment in a very different way from spheres;<sup>19,20</sup> in addition, they show novel packing/flow behavior on solid surfaces and in suspensions.<sup>21,22</sup> Our procedure combines this type of natural shape anisotropy with LCEs' ability to mechanically respond to changes in their environment (e.g., elongate on cooling), thus potentially paving the way for these objects to be used in applications such as micromuscles and microvalves.<sup>23</sup>

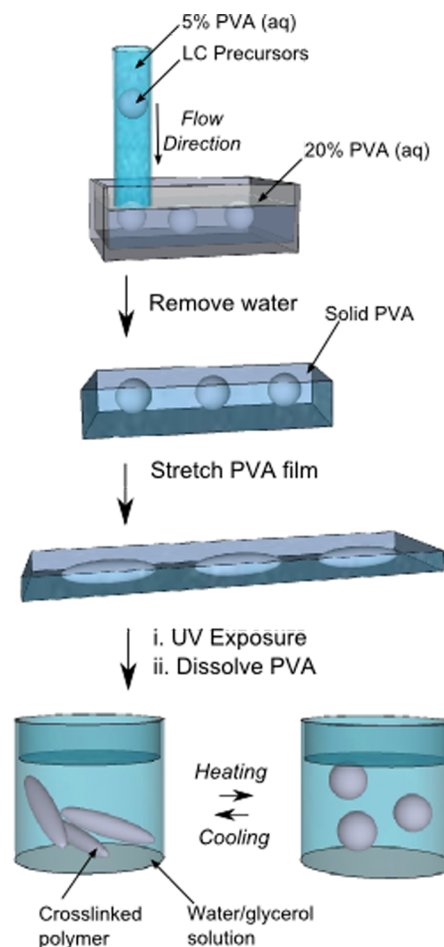
In this article, we demonstrate a method for the formation of ellipsoidal LCE micromuscles, highly anisotropic colloid particles with dimensions of the order of tens of micrometers, which reversibly expand and contract with temperature. We use a microfluidic device to break up liquid acrylate LCE monomer into droplets, a convenient method for the small amounts of liquid we used. (Emulsion methods could be employed to scale-up this process.) Then, we embed these droplets in a stretchable, thermoplastic polymer matrix. From this starting point, we demonstrate that many LCE micro-objects can be made at once. By mechanical stretching of the matrix followed by photopolymerization and cross-linking of the dispersed LC material, we form uniaxially aligned, highly anisotropic particles in a massively parallel way only limited by the physical size of the stretching polymer matrix. We demonstrate that the actuating strain achieved by these objects is comparable to macroscale actuators previously made (from the same acrylate mesogens) by the group of Keller.<sup>8</sup> The alignment achieved is the same, while notably, the synthetic procedure is simpler because confinement allows the elimination of the partial cross-linking step in previous mechanical alignment methods. In addition, this method rapidly creates multiple LCE micro-objects in parallel, thus allowing for scalability of the synthetic process.

## ■ RESULTS AND DISCUSSION

Microfluidics can be used to create uniform droplets of one phase in a continuously flowing second phase. We used a microfluidic channel to create uniform droplets of a polymer-

izable LC mesogen, in an aqueous solution of poly(vinyl alcohol) (PVA) (see Scheme 1).

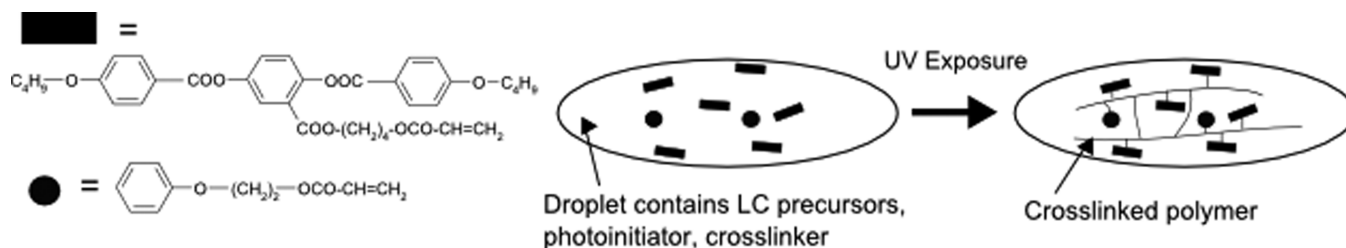
**Scheme 1. Scheme To Illustrate the Process Used to Form Anisotropic LCE Particles<sup>a</sup>**



<sup>a</sup>In a heated microfluidic channel, droplets of the LCE precursors are formed in a continuous phase consisting of 5% aqueous PVA with an added 5% SDS surfactant. As these droplets exit the microfluidic device, they are collected in a well filled with 20% aqueous PVA, thus forming stable droplets. Water is allowed to evaporate from the PVA solution, thus resulting in a solid PVA film containing discrete, spherical quantities of the LC precursors. This film is then heated to allow stretching of the material before being cooled to a temperature at which the PVA film is solid. The material is subsequently exposed to UV light in order to polymerize the LCE, before being immersed in water to dissolve the PVA, resulting in solid LCE objects that change shape with temperature.

Upon subsequent drying of the solution, the thermoplastic PVA polymer can be stretched, thus forcing the objects held within the matrix to adopt ellipsoidal shapes (as has previously been demonstrated by Ho et al. using polystyrene objects)<sup>24,25</sup> without the need for each object to be individually clamped. After the stretching process, the LCE precursor can be polymerized and cross-linked under UV irradiation, thus 'freezing in' the orientational order imposed on the LC during stretching (see Experimental section for further details on the procedure).

In microfluidic channels, the formation of droplets containing LCE precursors is problematic because the most

Scheme 2. Illustration of the Chemistry of the LC Precursors Used and Their Reaction to Form a Crosslinked Matrix<sup>a</sup>

<sup>a</sup>The LC monomer (4'-acryloyloxybutyl 2,5-(4'-butyloxybenzoyloxy)benzoate) consists of a rigid, anisotropic moiety (composed of three chemically bound aromatic rings) with an attached acrylate group. A second acrylate monomer (ethylene glycol phenyl ether acrylate) is added in order to lower the temperature at which this mixture is liquid and to reduce the nematic-isotropic transition point of the LC. In addition to these, a crosslinking diacrylate (1,6-hexanediol diacrylate) and a UV photoinitiator (benzoin methyl ether) must be added. After the formation of ellipsoidal objects (with an overall preferred direction of the LC groups) from these precursors, UV exposure causes the polymerization and crosslinking of the acrylates, thus fixing their topology.

commonly studied acrylate-containing LC mesogens are solid at room temperature. A heated microfluidic setup has previously been used to form such droplets (with the LC precursors in a molten state) in an oily carrier fluid.<sup>2,18</sup> We found that by using the same acrylate-containing mesogen (4'-acryloyloxybutyl 2,5-(4'-butyloxybenzoyloxy)benzoate), which displays an enantiotropic LC phase between 72 and 98 °C,<sup>8</sup> we can reduce the processing temperature even further by adding ethylene glycol phenyl ether acrylate to the LC monomer (see Scheme 2). This acrylate is commercially available, inexpensive, and liquid at room temperature; with its addition, the precursor mixture is liquid at 55–60 °C, which allows the droplets to be formed in an aqueous environment without rapid water evaporation. In addition to these two acrylates, a diacrylate (1,6-hexanediol diacrylate) is added as a cross-linker, along with a catalytic quantity of a UV photoinitiator, benzoin methyl ether (Sigma Aldrich). This initiator was chosen for its thermal stability, good match to available UV sources (maximum absorption at 250 nm), and the robust acrylate reactions seen with it.

In order to determine the properties of the LCE formed from the acrylate mixture, an initial bulk polymerization was carried out on 0.1 g of the material, using a 1:1 molar ratio of the LC acrylate to the non-LC acrylate (with an added 10 mol % of the cross-linker 1,6-hexanediol diacrylate and a catalytic quantity of the photoinitiator benzoin methyl ether). After a period of 1 h under UV irradiation, a solid material was formed, and the thermal behavior of this was characterized by differential scanning calorimetry (DSC) (see Figure 1 for the DSC trace). The DSC indicates that a nematic phase is formed at a temperature range of 43–58 °C; these data give us an indication of the temperature range, over which the LCE objects should spontaneously change shape.

In a heated microfluidic setup, it was possible to maintain a good flow of droplets within the chip, and to collect these in a viscous PVA solution to prevent their coalescence afterward. The PVA solution was subsequently dried, leaving behind a solid film containing spherical objects that are bright when viewed between crossed polarizers. This solid film was stretched while being subjected to a flow of hot air. Areas of the film near the ends were not uniformly stretched, due to the grips preventing contraction of the film ends in the perpendicular direction. Thus the ends and areas of the film that did not reach a strain of 200% were discarded. The film was subsequently cooled to 50 °C, so that the LC mesogens were held in the nematic phase, while the PVA remained solid

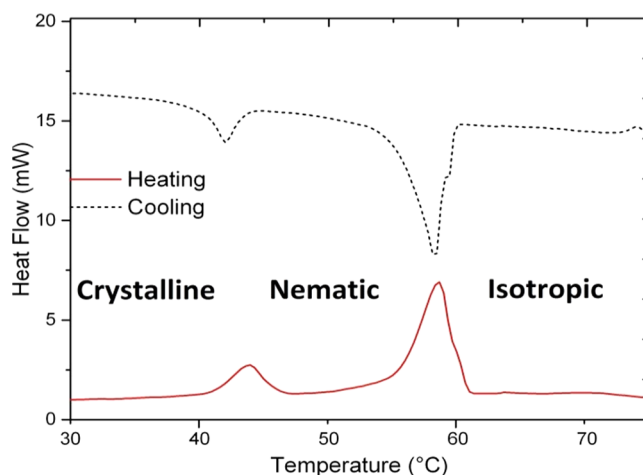


**Figure 1.** DSC trace taken from a bulk sample of 0.1 g of polymerized LCE. This material exhibits an enantiotropic phase change, with the nematic phase occurring between 43 and 58 °C during both the heating and the cooling steps. The DSC was run at a heating/cooling rate of 10 °C/min, against an air reference.

(PVA has a  $T_g$  of 80 °C and a melting point of 180 °C). Subsequent immersion in water dissolves the PVA, producing a dilute suspension of solid ellipsoidal polymer objects that was concentrated by centrifugation. Glycerol was added to this suspension, so that the LCE objects were held in a liquid that could easily be heated through the LC transition temperature with minimal evaporation of the solution, thus allowing the changing particle shape to be followed via optical microscopy.

After making microscale ellipsoids using our technique, we were able to investigate their properties. Figure 2 shows a series of optical micrographs taken as these objects were heated and cooled while suspended in a carrier fluid (glycerol); clear shape changes are evident. At the lower temperatures, the object is ellipsoidal and appears bright when viewed between crossed polarizers; as the temperature is increased, the aspect ratio of the ellipse is reduced, and the object eventually becomes dark (indicating that the nematic-isotropic transition has taken place). As temperature is lowered, the length of the object increases.

The shape change is both reversible and repeatable, as demonstrated in Figure 3a; this graph follows the length of an ellipsoid (along the long axis) over the course of several heating/cooling cycles. It is clear from these data that the particles reversibly contract along this axis during heating,



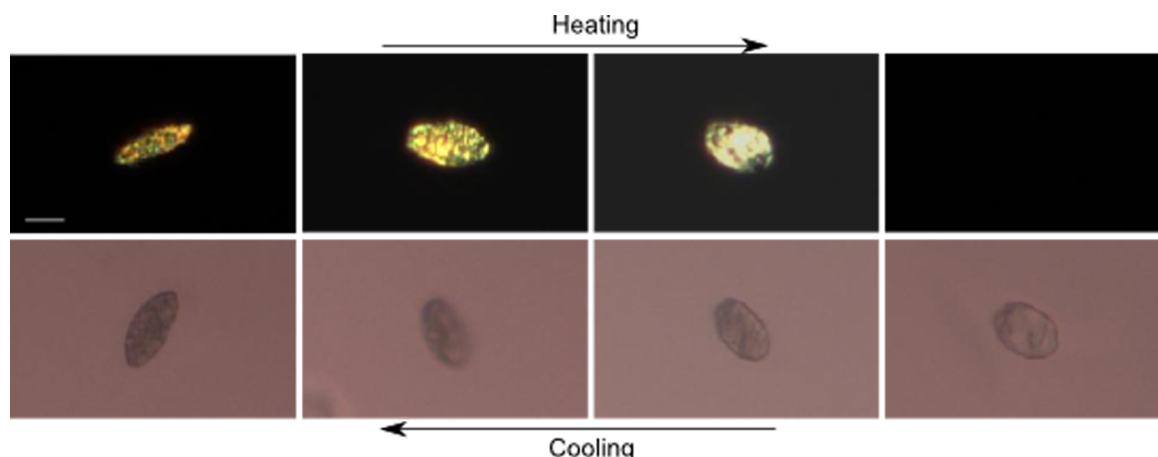


**Figure 2.** Optical micrographs illustrating the response of a typical particle when subjected to heating/cooling. The images in the top row were taken with the object between crossed polarizers, and illustrate the fact that the object contracts along its long axis during the heating process, before eventually becoming dark as the LC adopts the isotropic phase. The images in the second row were taken without crossed polarizers and illustrate the lengthening of the object as it is cooled. The scale bar represents 15  $\mu\text{m}$ .

before lengthening during the cooling phase. This behavior is analogous to the LCE contraction observed in films fabricated using the two-step stretching method, though the objects are micro- rather than macroscale. It is also important to note that only one cross-linking step has been employed during this process (whereas the standard two-step stretching method requires two); this is due to the fact that the LCE precursors are held within the PVA matrix and therefore do not need to be lightly cross-linked in order that they may be grasped for mechanical stretching. We infer, therefore, that the LC alignment is induced during the stretching process by the flow of LC mesogens and also by surface effects caused by the alignment of PVA chains. A similar phenomenon has previously been studied in (noncross-linked, low molecular weight) liquid crystals held within a stretched porous matrix;<sup>26,27</sup> these studies indicated that ordering of the liquid crystal was linked to the surface interaction between the LC mesogens and the matrix. LC alignment near rubbed surfaces depends on the anchoring strength of the surface,<sup>28</sup> and the thickness of the aligned layer can be of the order of tens of micrometers.<sup>29</sup> Since this is comparable to the diameter of our LCE objects, we expect surface effects to be significant.

It was often observed that the first heating cycle would result in a greater length change than subsequent cycles but after this the expansion/contraction becomes more consistent. We infer that the initial (large) change is due to the relaxation of a kinetically trapped structure achieved by stretching the precursor droplets and cooled into a nonequilibrium state. During further temperature cycling the changes are under thermodynamic control and the structural changes result in stable and reversible length changes; the LCE mesogen ordering changes from the nematic (longer) to the isotropic phase (shorter) and vice versa.

The maximum  $L/L_0$  of  $1.5 \pm 0.1$  is typical of monodomain bulk LCEs, with observed strain changes of  $(L_{\text{max}} - L_0)/L_0$  up to 30% (Figure 3b). In order to check that the contraction of the LCE object was indeed due to a LC phase change (and not a shorter projection due to accidental tumbling of the particle during the experiment) we verified that the thickness of the object also changed during the heating/cooling stage of the experiment. Using the volume of a symmetrical ellipsoid ( $V = 4/3\pi ab^2$ , where  $a$  and  $b$  are the major and minor axes of the

ellipsoid, respectively) and assuming a constant volume for each object, we can relate the length change of the object to its change in diameter. We thus verified that the increasing diameter of the object during heating was consistent with the trend shown for decreasing length (Figure 3b).

The maximum value of  $L/L_0$  seen for each particle (strain changes of  $\sim 30\%$ ) are indicative of good alignment of the nematic domains in the material. This value is in good agreement with that seen for the best bulk side-chain LCEs,<sup>9</sup> where alignment is achieved by careful balance between partial cross-linking and further reaction under extensional stress. Good alignment also results in higher applied stresses, we have measured stresses of  $\sim 30$  kPa exerted by films we have synthesized from similar side-chain elastomers.<sup>4</sup>

In our system the mesogen-containing chains align during shear and extensional alignment of the droplets to ellipsoids, after which the order is maintained without cross-linking due to the small thickness of the objects ( $<20$   $\mu\text{m}$ ) confining the mesogens to a volume where all distances to a surface are less than the surface alignment length. Such high degree of alignment is achieved in a single-step reaction, greatly increasing the possibilities for fabrication reproducibility and reaction control in LCE materials. Using main-chain LCEs is a promising direction for extending this technique, where strain changes of up to 500% are possible with alignment. We hope our scalable and simplified synthetic method for generating micromuscles with such properties will be a reliable route for creating microactuators with stress-strain characteristics approaching those of typical biological muscles.<sup>30</sup>

In summary, we have demonstrated a novel method for the creation of monodomain, microscale LCE objects with in-built anisotropy. These objects display favorable stress/strain behavior, in that they can contract uniaxially upon heating, with a strain change similar to that shown by bulk examples of side-chain acrylate LCEs. Their potential application as microactuators is further favored by the fact that they are self-contained and do not require an aqueous environment in which to expand/contract, as hydrogel actuators do. This allows their use in space and in water-sensitive devices.

Most importantly, the objects we have made are ellipsoidal, thus giving an anisotropic shape-changing behavior unlike that seen in previous studies, and the process for their fabrication is

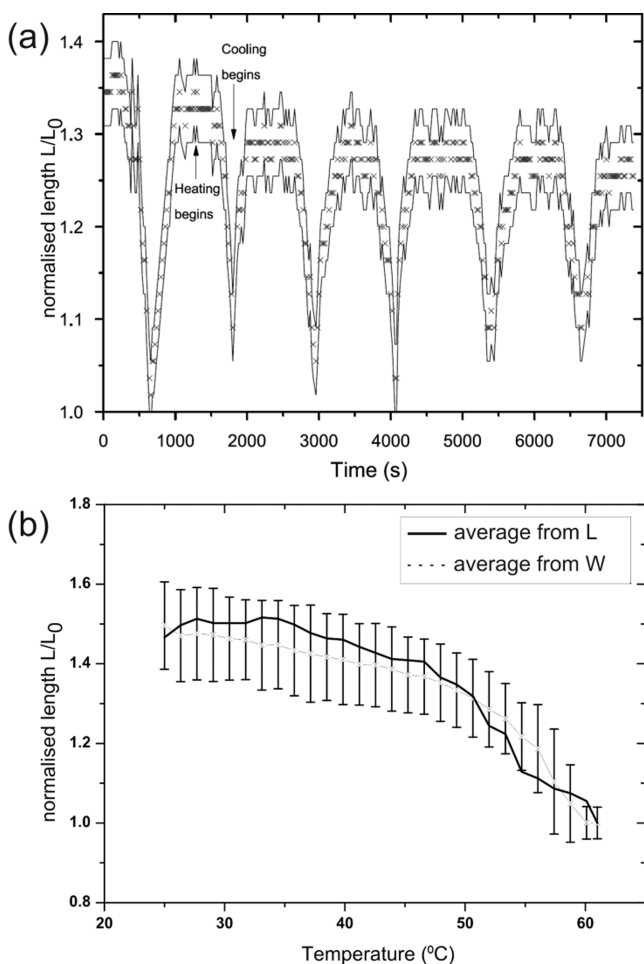


**Figure 3.** (a) Graph to show the length change of one particle measured over several cycles of heating and cooling. An optical image was taken every 20 s during the process, and the length of the object was measured; the length is shown as the length  $L$  (at time  $T$ ) divided by  $L_0$  (the shortest length achieved by the object, at high temperatures). Crosses on the graph indicate the length measured on each image, and the continuous lines represent the upper and lower error bounds on this measurement, assuming an error in the image analysis of  $\pm 1$  pixel. (b) Graph showing average length change with temperature. Measurements were taken from particles that had already been heated and cooled at least once, in order to show only the thermodynamic reversible length change seen on heating/cooling cycles after the first one. Length normalized by the shortest length ( $L_0$ ).

scalable. The high degree of alignment observed in the micro-ellipsoids is can be achieved without initial partial cross-linking, due to confinement effects, which opens the door for easier design and fabrication of microactuators.

## EXPERIMENTAL SECTION

**LCE Precursors.** 4'-acryloyloxybutyl 2,5-(4'-butyloxybenzoyloxy)-benzoate was synthesized as described by Thomsen et al.<sup>8</sup> Ethylene glycol phenyl ether acrylate, benzoin methyl ether, 1,6-hexanediol diacrylate, and PVA were obtained from Sigma-Aldrich and used as received.

**Preparation of Microfluidic Devices.** Microfluidic devices were prepared by conventional soft lithography. Channels of the design shown in Supporting Information Figure 1 were printed on a transparency (Circuit Graphics) at high resolution. Silicon wafers were spincoated with photoresist SU-8 3050 (Microchem) to 50  $\mu\text{m}$  thickness and exposed to UV light through the transparency.

Unexposed photoresist was removed by dissolution in 1-methoxy-2-propyl acetate (Sigma Aldrich). Sylgard 184 poly(dimethyl siloxane) (PDMS) elastomer kit (Dow Corning) was cured at 10:1 ratio on top of the patterned wafer. The PDMS was cut from the mold and holes punched for inlet tubing using a 1 mm biopsy punch (Kai Industries). Immediately before use, the PDMS was exposed to oxygen plasma in a Femto plasma asher (Diener Electronics) to bond it to a glass slide and leave the surface hydrophilic. The channels were filled with water until use.

**Microfluidic Device Operation.** A homemade heated microfluidic setup is used. The continuous and dispersed phases are injected into the hydrophilic device from glass syringes (VWR International) via polyethylene tubing (SLS). Flow rates are controlled by syringe pumps (Harvard Apparatus) at 500  $\mu\text{L/h}$  for the continuous phase and 200  $\mu\text{L/h}$  for the dispersed phase. The continuous phase consists of an aqueous solution of 5% PVA, 5% sodium dodecyl sulphate (SDS) (by mass). The dispersed phase consists of a 45:45:10 molar ratio of 4'-acryloyloxybutyl 2,5-(4'-butyloxybenzoyloxy)benzoate, ethylene glycol phenyl ether acrylate, and 1,6-hexanediol diacrylate; to this mixture, a catalytic quantity of benzoin methyl ether is added, and the mixture is warmed gently to form a liquid.

**Creation of Anisotropic LCE Particles.** The LCE precursor droplets, dispersed within the aqueous PVA solution, were collected into a well containing more concentrated (20% by mass) PVA. Water within the PVA solution was then allowed to evaporate, leaving a solid film containing LCE objects that appear bright under crossed polarisers. The film was marked into rectangles, each of size  $1 \times 0.5$  cm, and stretched under a flow of hot air; any part of the material where the rectangles had not stretched to 200% of their original length was discarded. The stretched film was held at 50  $^{\circ}\text{C}$  and subjected to irradiation by ultraviolet light (254 nm, 100 W) for a period of 1 h, before being immersed in water for several hours to dissolve the PVA, and then subjected to centrifugation (5 min, 1000 rpm) in order to concentrate the resulting suspended LCE objects. Drops of this suspension were mixed with glycerol and placed on microscope slides so that their behavior could be imaged as their surrounding temperature was raised and lowered.

## ASSOCIATED CONTENT

### Supporting Information

Design for the microfluidic channels used for fabricating the droplets. This material is available free of charge via the Internet at <http://pubs.acs.org>.

## AUTHOR INFORMATION

### Corresponding Author

sks46@cam.ac.uk

### Notes

The authors declare no competing financial interest.

## ACKNOWLEDGMENTS

This work was funded by the European research council (ERC) grant EMATTER (no. 280078), and EPSRC studentship for S.G.

## REFERENCES

- (1) Terentjev, E. M.; Warner, M. *Liquid Crystal Elastomers*; Oxford University Press: Oxford, 2007.
- (2) Ohm, C.; Brehmer, M.; Zentel, R. *Adv. Mater.* **2010**, *22*, 3366–3387.
- (3) Ahir, S. V.; Tajbakhsh, A. R.; Terentjev, E. M. *Adv. Funct. Mater.* **2006**, *16*, 556–560.
- (4) Tajbakhsh, A. R.; Terentjev, E. M. *Eur. Phys. J. E: Soft Matter Biol. Phys.* **2001**, *6*, 181–188.
- (5) Jiang, H.; Li, C.; Huang, X. *Nanoscale* **2013**, *5*, 5225–5240.
- (6) Spillmann, C. M.; Naciri, J.; Martin, B. D.; Farahat, W.; Herr, H.; Ratna, B. R. *Sens. Actuators, A* **2007**, *133*, 500–505.

- (7) Camargo, C. J.; Campanella, H.; Marshall, J. E.; Torras, N.; Zinoviev, K.; Terentjev, E. M.; Esteve, J. *Macromol. Rapid Commun.* **2011**, *32*, 1953–1959.
- (8) Thomsen, D. L.; Keller, P.; Naciri, J.; Pink, R.; Jeon, H.; Shenoy, D.; Ratna, B. R. *Macromolecules* **2001**, *34*, 5868–5875.
- (9) Küpfer, J.; Finkelmann, H. *Makromol. Chem., Rapid Comm.* **1991**, *12*, 717–726.
- (10) Buguin, A.; Li, M.-H.; Silberzan, P.; Ladoux, B.; Keller, P. *J. Am. Chem. Soc.* **2006**, *128*, 1088–1089.
- (11) Boamfa, M. I.; Lazarenko, S. V.; Vermolen, E. C. M.; Kirilyuk, A.; Rasing, T. *Adv. Mater.* **2005**, *17*, 610–614.
- (12) Freedericksz, V.; Zolina, V. *Trans. Faraday Soc.* **1933**, *29*, 919–930.
- (13) Sánchez-Ferrer, A.; Fischl, T.; Stubenrauch, M.; Wurmus, H.; Hoffmann, M.; Finkelmann, H. *Macromol. Chem. Phys.* **2009**, *210*, 1671–1677.
- (14) Van Oosten, C. L.; Bastiaansen, C. W. M.; Broer, D. J. *Nat. Mater.* **2009**, *8*, 677–682.
- (15) Sousa, M. E.; Broer, D. J.; Bastiaansen, C. W. M.; Freund, L. B.; Crawford, G. P. *Adv. Mater.* **2006**, *18*, 1842–1845.
- (16) Elias, A. L.; Harris, K. D.; Bastiaansen, C. W. M.; Broer, D. J.; Brett, M. J. *J. Mater. Chem.* **2006**, *16*, 2903–2912.
- (17) Van der Zande, B. M. I.; Steenbakkers, J.; Lub, J.; Leewis, C. M.; Broer, D. J. *J. Appl. Phys.* **2005**, *97*, 123519.
- (18) Ohm, C.; Serra, C.; Zentel, R. *Adv. Mater.* **2009**, *21*, 4859–4862.
- (19) Dusenbery, D. B. *Living at Micro Scale: The Unexpected Physics of Being Small*; Harvard University Press, 2011.
- (20) Thompson, A. J.; Mastria, E. M.; Eniola-Adefeso, O. *Biomaterials* **2013**, *34*, 5863–5871.
- (21) Skjeltorp, A. T.; Ugelstad, J.; Ellingsen, T. *J. Colloid Interface Sci.* **1986**, *113*, 577–582.
- (22) Nussinovitch, A. *Polymer Macro- and Micro-Gel Beads: Fundamentals and Applications*; Springer: New York, 2010.
- (23) Fleischmann, E.-K.; Liang, H.-L.; Kapernaum, N.; Giesselmann, F.; Lagerwall, J.; Zentel, R. *Nat. Commun.* **2012**, *3*, 1178.
- (24) Ho, C. C.; Keller, A.; Odell, J. A.; Ottewill, R. H. *Colloid Polym. Sci.* **1993**, *271*, 469–479.
- (25) Ho, C. C.; Ottewill, R. H.; Keller, A.; Odell, J. A. *Polym. Int.* **1993**, *30*, 207–211.
- (26) Amimori, I.; Eakin, J. N.; Qi, J.; Skacej, G.; Zumer, S.; Crawford, G. P. *Phys. Rev. E* **2005**, *71*, 031702.
- (27) Fujikake, H.; Kuboki, M.; Murashige, T.; Sato, H.; Kikuchi, H.; Kurita, T. *J. Appl. Phys.* **2003**, *94*, 2864.
- (28) De Gennes, P. G. *The Physics of Liquid Crystals*; Oxford University Press: Oxford, 1995.
- (29) Barbero, G.; Madhusudana, N. V.; Durand, G. *J. Phys., Lett.* **1984**, *45*, L613–L619.
- (30) Huber, J. E.; Fleck, N. A.; Ashby, M. F. *Proc. R. Soc. London, Ser. A* **1997**, *453*, 2185–2205.